Measurement of the Ratio $\mathcal{B}(B^- \to D^{*0}K^-)/\mathcal{B}(B^- \to D^{*0}\pi^-)$ and the CP-asymmetry of $B^- \to D^{*0}_{CP+}K^-$ decays with the BABAR detector

The BABAR Collaboration

August 14, 2004

Abstract

We present a study of the decays $B^- \to D^{*0}\pi^-$ and $B^- \to D^{*0}K^-$, where the D^{*0} decays into $D^0\pi^0$, with the D^0 reconstructed in the CP eigenstates K^-K^+ and $\pi^-\pi^+$ and in the (non-CP) channels $K^-\pi^+$, $K^-\pi^+\pi^+\pi^-$, and $K^-\pi^+\pi^0$. We use an unbinned maximum likelihood fit to measure the signal yields. Using a sample of about 123 million $\Upsilon(4S)$ decays into $B\overline{B}$ pairs, we measure the ratios of decay rates

$$R^*_{CP+} \equiv \frac{\mathcal{B}(B^- \to D^{*0}_{CP+}K^-)}{\mathcal{B}(B^- \to D^{*0}_{CP+}\pi^-)} = 0.088 \pm 0.021(\text{stat})^{+0.007}_{-0.005}(\text{syst}),$$

and provide the first measurements of

$$R^*_{\text{non}-CP} \equiv \frac{\mathcal{B}(B^- \to D^{*0}_{\text{non}-CP}K^-)}{\mathcal{B}(B^- \to D^{*0}_{\text{non}-CP}\pi^-)} = 0.0805 \pm 0.0040(\text{stat})^{+0.0039}_{-0.0032}(\text{syst}),$$

and of the CP asymmetry

$$A^*_{CP+} \equiv \frac{\mathcal{B}(B^- \to D^{*0}_{CP+}K^-) - \mathcal{B}(B^+ \to D^{*0}_{CP+}K^+)}{\mathcal{B}(B^- \to D^{*0}_{CP+}K^-) + \mathcal{B}(B^+ \to D^{*0}_{CP+}K^+)} = -0.02 \pm 0.24(\text{stat}) \pm 0.05(\text{syst}).$$

These results are preliminary.

Submitted to the 32$^{\text{nd}}$ International Conference on High-Energy Physics, ICHEP 04,
16 August—22 August 2004, Beijing, China

The *BABAR* Collaboration,

B. Aubert, R. Barate, D. Boutigny, F. Couderc, J.-M. Gaillard, A. Hicheur, Y. Karyotakis, J. P. Lees,
V. Tisserand, A. Zghiche

Laboratoire de Physique des Particules, F-74941 Annecy-le-Vieux, France

A. Palano, A. Pompili

Università di Bari, Dipartimento di Fisica and INFN, I-70126 Bari, Italy

J. C. Chen, N. D. Qi, G. Rong, P. Wang, Y. S. Zhu

Institute of High Energy Physics, Beijing 100039, China

G. Eigen, I. Ofte, B. Stugu

University of Bergen, Inst. of Physics, N-5007 Bergen, Norway

G. S. Abrams, A. W. Borgland, A. B. Breon, D. N. Brown, J. Button-Shafer, R. N. Cahn, E. Charles,
C. T. Day, M. S. Gill, A. V. Gritsan, Y. Groysman, R. G. Jacobsen, R. W. Kadel, J. Kadyk, L. T. Kerth,
Yu. G. Kolomensky, G. Kukartsev, G. Lynch, L. M. Mir, P. J. Oddone, T. J. Orimoto, M. Pripstein,
N. A. Roe, M. T. Ronan, V. G. Shelkov, W. A. Wenzel

Lawrence Berkeley National Laboratory and University of California, Berkeley, CA 94720, USA

M. Barrett, K. E. Ford, T. J. Harrison, A. J. Hart, C. M. Hawkes, S. E. Morgan, A. T. Watson

University of Birmingham, Birmingham, B15 2TT, United Kingdom

M. Fritsch, K. Goetzen, T. Held, H. Koch, B. Lewandowski, M. Pelizaeus, M. Steinke

Ruhr Universität Bochum, Institut für Experimentalphysik 1, D-44780 Bochum, Germany

J. T. Boyd, N. Chevalier, W. N. Cottingham, M. P. Kelly, T. E. Latham, F. F. Wilson

University of Bristol, Bristol BS8 1TL, United Kingdom

T. Cuhadar-Donszelmann, C. Hearty, N. S. Knecht, T. S. Mattison, J. A. McKenna, D. Thiessen

University of British Columbia, Vancouver, BC, Canada V6T 1Z1

A. Khan, P. Kyberd, L. Teodorescu

Brunel University, Uxbridge, Middlesex UB8 3PH, United Kingdom

A. E. Blinov, V. E. Blinov, V. P. Druzhinin, V. B. Golubev, V. N. Ivanchenko, E. A. Kravchenko,
A. P. Onuchin, S. I. Serednyakov, Yu. I. Skovpen, E. P. Solodov, A. N. Yushkov

Budker Institute of Nuclear Physics, Novosibirsk 630090, Russia

D. Best, M. Bruinsma, M. Chao, I. Eschrich, D. Kirkby, A. J. Lankford, M. Mandelkern, R. K. Mommsen,
W. Roethel, D. P. Stoker

University of California at Irvine, Irvine, CA 92697, USA

C. Buchanan, B. L. Hartfiel

University of California at Los Angeles, Los Angeles, CA 90024, USA

S. D. Foulkes, J. W. Gary, B. C. Shen, K. Wang

University of California at Riverside, Riverside, CA 92521, USA

D. del Re, H. K. Hadavand, E. J. Hill, D. B. MacFarlane, H. P. Paar, Sh. Rahatlou, V. Sharma

University of California at San Diego, La Jolla, CA 92093, USA

J. W. Berryhill, C. Campagnari, B. Dahmes, O. Long, A. Lu, M. A. Mazur, J. D. Richman, W. Verkerke

University of California at Santa Barbara, Santa Barbara, CA 93106, USA

T. W. Beck, A. M. Eisner, C. A. Heusch, J. Kroseberg, W. S. Lockman, G. Nesom, T. Schalk,
B. A. Schumm, A. Seiden, P. Spradlin, D. C. Williams, M. G. Wilson

University of California at Santa Cruz, Institute for Particle Physics, Santa Cruz, CA 95064, USA

J. Albert, E. Chen, G. P. Dubois-Felsmann, A. Dvoretskii, D. G. Hitlin, I. Narsky, T. Piatenko,
F. C. Porter, A. Ryd, A. Samuel, S. Yang

California Institute of Technology, Pasadena, CA 91125, USA

S. Jayatilleke, G. Mancinelli, B. T. Meadows, M. D. Sokoloff

University of Cincinnati, Cincinnati, OH 45221, USA

T. Abe, F. Blanc, P. Bloom, S. Chen, W. T. Ford, U. Nauenberg, A. Olivas, P. Rankin, J. G. Smith,
J. Zhang, L. Zhang

University of Colorado, Boulder, CO 80309, USA

A. Chen, J. L. Harton, A. Soffer, W. H. Toki, R. J. Wilson, Q. Zeng

Colorado State University, Fort Collins, CO 80523, USA

D. Altenburg, T. Brandt, J. Brose, M. Dickopp, E. Feltresi, A. Hauke, H. M. Lacker, R. Müller-Pfefferkorn,
R. Nogowski, S. Otto, A. Petzold, J. Schubert, K. R. Schubert, R. Schwierz, B. Spaan, J. E. Sundermann

Technische Universität Dresden, Institut für Kern- und Teilchenphysik, D-01062 Dresden, Germany

D. Bernard, G. R. Bonneaud, F. Brochard, P. Grenier, S. Schrenk, Ch. Thiebaux, G. Vasileiadis, M. Verderi

Ecole Polytechnique, LLR, F-91128 Palaiseau, France

D. J. Bard, P. J. Clark, D. Lavin, F. Muheim, S. Playfer, Y. Xie

University of Edinburgh, Edinburgh EH9 3JZ, United Kingdom

M. Andreotti, V. Azzolini, D. Bettoni, C. Bozzi, R. Calabrese, G. Cibinetto, E. Luppi, M. Negrini,
L. Piemontese, A. Sarti

Università di Ferrara, Dipartimento di Fisica and INFN, I-44100 Ferrara, Italy

E. Treadwell

Florida A&M University, Tallahassee, FL 32307, USA

F. Anulli, R. Baldini-Ferroli, A. Calcaterra, R. de Sangro, G. Finocchiaro, P. Patteri, I. M. Peruzzi,
M. Piccolo, A. Zallo

Laboratori Nazionali di Frascati dell'INFN, I-00044 Frascati, Italy

A. Buzzo, R. Capra, R. Contri, G. Crosetti, M. Lo Vetere, M. Macri, M. R. Monge, S. Passaggio,
C. Patrignani, E. Robutti, A. Santroni, S. Tosi

Università di Genova, Dipartimento di Fisica and INFN, I-16146 Genova, Italy

S. Bailey, G. Brandenburg, K. S. Chaisanguanthum, M. Morii, E. Won

Harvard University, Cambridge, MA 02138, USA

3

R. S. Dubitzky, U. Langenegger

Universität Heidelberg, Physikalisches Institut, Philosophenweg 12, D-69120 Heidelberg, Germany

W. Bhimji, D. A. Bowerman, P. D. Dauncey, U. Egede, J. R. Gaillard, G. W. Morton, J. A. Nash, M. B. Nikolich, G. P. Taylor

Imperial College London, London, SW7 2AZ, United Kingdom

M. J. Charles, G. J. Grenier, U. Mallik

University of Iowa, Iowa City, IA 52242, USA

J. Cochran, H. B. Crawley, J. Lamsa, W. T. Meyer, S. Prell, E. I. Rosenberg, A. E. Rubin, J. Yi

Iowa State University, Ames, IA 50011-3160, USA

M. Biasini, R. Covarelli, M. Pioppi

Università di Perugia, Dipartimento di Fisica and INFN, I-06100 Perugia, Italy

M. Davier, X. Giroux, G. Grosdidier, A. Höcker, S. Laplace, F. Le Diberder, V. Lepeltier, A. M. Lutz, T. C. Petersen, S. Plaszczynski, M. H. Schune, L. Tantot, G. Wormser

Laboratoire de l'Accélérateur Linéaire, F-91898 Orsay, France

C. H. Cheng, D. J. Lange, M. C. Simani, D. M. Wright

Lawrence Livermore National Laboratory, Livermore, CA 94550, USA

A. J. Bevan, C. A. Chavez, J. P. Coleman, I. J. Forster, J. R. Fry, E. Gabathuler, R. Gamet, D. E. Hutchcroft, R. J. Parry, D. J. Payne, R. J. Sloane, C. Touramanis

University of Liverpool, Liverpool L69 7ZE, United Kingdom

J. J. Back,[1] C. M. Cormack, P. F. Harrison,[1] F. Di Lodovico, G. B. Mohanty[1]

Queen Mary, University of London, E1 4NS, United Kingdom

C. L. Brown, G. Cowan, R. L. Flack, H. U. Flaecher, M. G. Green, P. S. Jackson, T. R. McMahon, S. Ricciardi, F. Salvatore, M. A. Winter

University of London, Royal Holloway and Bedford New College, Egham, Surrey TW20 0EX, United Kingdom

D. Brown, C. L. Davis

University of Louisville, Louisville, KY 40292, USA

J. Allison, N. R. Barlow, R. J. Barlow, P. A. Hart, M. C. Hodgkinson, G. D. Lafferty, A. J. Lyon, J. C. Williams

University of Manchester, Manchester M13 9PL, United Kingdom

A. Farbin, W. D. Hulsbergen, A. Jawahery, D. Kovalskyi, C. K. Lae, V. Lillard, D. A. Roberts

University of Maryland, College Park, MD 20742, USA

G. Blaylock, C. Dallapiccola, K. T. Flood, S. S. Hertzbach, R. Kofler, V. B. Koptchev, T. B. Moore, S. Saremi, H. Staengle, S. Willocq

University of Massachusetts, Amherst, MA 01003, USA

[1]Now at Department of Physics, University of Warwick, Coventry, United Kingdom

4

R. Cowan, G. Sciolla, S. J. Sekula, F. Taylor, R. K. Yamamoto

Massachusetts Institute of Technology, Laboratory for Nuclear Science, Cambridge, MA 02139, USA

D. J. J. Mangeol, P. M. Patel, S. H. Robertson

McGill University, Montréal, QC, Canada H3A 2T8

A. Lazzaro, V. Lombardo, F. Palombo

Università di Milano, Dipartimento di Fisica and INFN, I-20133 Milano, Italy

J. M. Bauer, L. Cremaldi, V. Eschenburg, R. Godang, R. Kroeger, J. Reidy, D. A. Sanders, D. J. Summers, H. W. Zhao

University of Mississippi, University, MS 38677, USA

S. Brunet, D. Côté, P. Taras

Université de Montréal, Laboratoire René J. A. Lévesque, Montréal, QC, Canada H3C 3J7

H. Nicholson

Mount Holyoke College, South Hadley, MA 01075, USA

N. Cavallo,[2] F. Fabozzi,[2] C. Gatto, L. Lista, D. Monorchio, P. Paolucci, D. Piccolo, C. Sciacca

Università di Napoli Federico II, Dipartimento di Scienze Fisiche and INFN, I-80126, Napoli, Italy

M. Baak, H. Bulten, G. Raven, H. L. Snoek, L. Wilden

NIKHEF, National Institute for Nuclear Physics and High Energy Physics, NL-1009 DB Amsterdam, The Netherlands

C. P. Jessop, J. M. LoSecco

University of Notre Dame, Notre Dame, IN 46556, USA

T. Allmendinger, K. K. Gan, K. Honscheid, D. Hufnagel, H. Kagan, R. Kass, T. Pulliam, A. M. Rahimi, R. Ter-Antonyan, Q. K. Wong

Ohio State University, Columbus, OH 43210, USA

J. Brau, R. Frey, O. Igonkina, C. T. Potter, N. B. Sinev, D. Strom, E. Torrence

University of Oregon, Eugene, OR 97403, USA

F. Colecchia, A. Dorigo, F. Galeazzi, M. Margoni, M. Morandin, M. Posocco, M. Rotondo, F. Simonetto, R. Stroili, G. Tiozzo, C. Voci

Università di Padova, Dipartimento di Fisica and INFN, I-35131 Padova, Italy

M. Benayoun, H. Briand, J. Chauveau, P. David, Ch. de la Vaissière, L. Del Buono, O. Hamon, M. J. J. John, Ph. Leruste, J. Malcles, J. Ocariz, M. Pivk, L. Roos, S. T'Jampens, G. Therin

Universités Paris VI et VII, Laboratoire de Physique Nucléaire et de Hautes Energies, F-75252 Paris, France

P. F. Manfredi, V. Re

Università di Pavia, Dipartimento di Elettronica and INFN, I-27100 Pavia, Italy

---

[2]Also with Università della Basilicata, Potenza, Italy

P. K. Behera, L. Gladney, Q. H. Guo, J. Panetta

University of Pennsylvania, Philadelphia, PA 19104, USA

C. Angelini, G. Batignani, S. Bettarini, M. Bondioli, F. Bucci, G. Calderini, M. Carpinelli, F. Forti,
M. A. Giorgi, A. Lusiani, G. Marchiori, F. Martinez-Vidal,[3] M. Morganti, N. Neri, E. Paoloni, M. Rama,
G. Rizzo, F. Sandrelli, J. Walsh

Università di Pisa, Dipartimento di Fisica, Scuola Normale Superiore and INFN, I-56127 Pisa, Italy

M. Haire, D. Judd, K. Paick, D. E. Wagoner

Prairie View A&M University, Prairie View, TX 77446, USA

N. Danielson, P. Elmer, Y. P. Lau, C. Lu, V. Miftakov, J. Olsen, A. J. S. Smith, A. V. Telnov

Princeton University, Princeton, NJ 08544, USA

F. Bellini, G. Cavoto,[4] R. Faccini, F. Ferrarotto, F. Ferroni, M. Gaspero, L. Li Gioi, M. A. Mazzoni,
S. Morganti, M. Pierini, G. Piredda, F. Safai Tehrani, C. Voena

Università di Roma La Sapienza, Dipartimento di Fisica and INFN, I-00185 Roma, Italy

S. Christ, G. Wagner, R. Waldi

Universität Rostock, D-18051 Rostock, Germany

T. Adye, N. De Groot, B. Franek, N. I. Geddes, G. P. Gopal, E. O. Olaiya

Rutherford Appleton Laboratory, Chilton, Didcot, Oxon, OX11 0QX, United Kingdom

R. Aleksan, S. Emery, A. Gaidot, S. F. Ganzhur, P.-F. Giraud, G. Hamel de Monchenault, W. Kozanecki,
M. Legendre, G. W. London, B. Mayer, G. Schott, G. Vasseur, Ch. Yèche, M. Zito

DSM/Dapnia, CEA/Saclay, F-91191 Gif-sur-Yvette, France

M. V. Purohit, A. W. Weidemann, J. R. Wilson, F. X. Yumiceva

University of South Carolina, Columbia, SC 29208, USA

D. Aston, R. Bartoldus, N. Berger, A. M. Boyarski, O. L. Buchmueller, R. Claus, M. R. Convery,
M. Cristinziani, G. De Nardo, D. Dong, J. Dorfan, D. Dujmic, W. Dunwoodie, E. E. Elsen, S. Fan,
R. C. Field, T. Glanzman, S. J. Gowdy, T. Hadig, V. Halyo, C. Hast, T. Hryn'ova, W. R. Innes,
M. H. Kelsey, P. Kim, M. L. Kocian, D. W. G. S. Leith, J. Libby, S. Luitz, V. Luth, H. L. Lynch,
H. Marsiske, R. Messner, D. R. Muller, C. P. O'Grady, V. E. Ozcan, A. Perazzo, M. Perl, S. Petrak,
B. N. Ratcliff, A. Roodman, A. A. Salnikov, R. H. Schindler, J. Schwiening, G. Simi, A. Snyder, A. Soha,
J. Stelzer, D. Su, M. K. Sullivan, J. Va'vra, S. R. Wagner, M. Weaver, A. J. R. Weinstein,
W. J. Wisniewski, M. Wittgen, D. H. Wright, A. K. Yarritu, C. C. Young

Stanford Linear Accelerator Center, Stanford, CA 94309, USA

P. R. Burchat, A. J. Edwards, T. I. Meyer, B. A. Petersen, C. Roat

Stanford University, Stanford, CA 94305-4060, USA

S. Ahmed, M. S. Alam, J. A. Ernst, M. A. Saeed, M. Saleem, F. R. Wappler

State University of New York, Albany, NY 12222, USA

[3]Also with IFIC, Instituto de Física Corpuscular, CSIC-Universidad de Valencia, Valencia, Spain
[4]Also with Princeton University, Princeton, USA

W. Bugg, M. Krishnamurthy, S. M. Spanier

University of Tennessee, Knoxville, TN 37996, USA

R. Eckmann, H. Kim, J. L. Ritchie, A. Satpathy, R. F. Schwitters

University of Texas at Austin, Austin, TX 78712, USA

J. M. Izen, I. Kitayama, X. C. Lou, S. Ye

University of Texas at Dallas, Richardson, TX 75083, USA

F. Bianchi, M. Bona, F. Gallo, D. Gamba

Università di Torino, Dipartimento di Fisica Sperimentale and INFN, I-10125 Torino, Italy

L. Bosisio, C. Cartaro, F. Cossutti, G. Della Ricca, S. Dittongo, S. Grancagnolo, L. Lanceri, P. Poropat,[5]
L. Vitale, G. Vuagnin

Università di Trieste, Dipartimento di Fisica and INFN, I-34127 Trieste, Italy

R. S. Panvini

Vanderbilt University, Nashville, TN 37235, USA

Sw. Banerjee, C. M. Brown, D. Fortin, P. D. Jackson, R. Kowalewski, J. M. Roney, R. J. Sobie

University of Victoria, Victoria, BC, Canada V8W 3P6

H. R. Band, B. Cheng, S. Dasu, M. Datta, A. M. Eichenbaum, M. Graham, J. J. Hollar, J. R. Johnson,
P. E. Kutter, H. Li, R. Liu, A. Mihalyi, A. K. Mohapatra, Y. Pan, R. Prepost, P. Tan, J. H. von
Wimmersperg-Toeller, J. Wu, S. L. Wu, Z. Yu

University of Wisconsin, Madison, WI 53706, USA

M. G. Greene, H. Neal

Yale University, New Haven, CT 06511, USA

---

[5]Deceased

7

1   INTRODUCTION

The study of $B^- \to D^{(*)0}K^{(*)-}$ decays will play an important role in our understanding of CP violation, as they can be used to constrain the angle $\gamma = \arg(-V_{ud}V_{ub}^*/V_{cd}V_{cb}^*)$ of the Cabibbo-Kobayashi-Maskawa (CKM) matrix in a theoretically clean way by exploiting the interference between the $b \to c\overline{u}s$ and $b \to u\overline{c}s$ decay amplitudes [1]. In the Standard Model, in the absence of $D^0\overline{D^0}$ mixing, $R_{CP\pm}^*/R_{\mathrm{non}-CP}^* \simeq 1 + r^2 \pm 2r\cos\delta\cos\gamma$, where

$$R_{\mathrm{non}-CP/CP\pm}^* \equiv \frac{\mathcal{B}(B^- \to D_{\mathrm{non}-CP/CP\pm}^{*0}K^-)}{\mathcal{B}(B^- \to D_{\mathrm{non}-CP/CP\pm}^{*0}\pi^-)},$$

r is the ratio of the color suppressed $B^+ \to D^{*0}K^+$ and color allowed $B^- \to D^{*0}K^-$ amplitudes ($r \sim 0.1 - 0.3$), and δ is the CP-conserving strong phase difference between those amplitudes. Furthermore, defining the direct CP asymmetry

$$A_{CP\pm}^* \equiv \frac{\mathcal{B}(B^- \to D_{CP\pm}^{*0}K^-) - \mathcal{B}(B^+ \to D_{CP\pm}^{*0}K^+)}{\mathcal{B}(B^- \to D_{CP\pm}^{*0}K^-) + \mathcal{B}(B^+ \to D_{CP\pm}^{*0}K^+)}, \tag{1}$$

we have: $A_{CP\pm}^* = \pm 2r\sin\delta\sin\gamma/(1 + r^2 \pm 2r\cos\delta\cos\gamma)$. The unknowns δ, r, and γ can be constrained from the measurements of $R_{\mathrm{non}-CP}^*$, $R_{CP\pm}^*$, and $A_{CP\pm}^*$. The Belle Collaboration has reported $R_{\mathrm{non}-CP}^* = 0.078 \pm 0.019 \pm 0.009$ using 10.1 fb^{-1} of data [2].

2   THE *BABAR* DETECTOR AND DATASET

We present the measurement of $R_{\mathrm{non}-CP}^*$, R_{CP+}^* and A_{CP+}^* performed using 113 fb^{-1} of data taken at the $\Upsilon(4S)$ resonance by the *BABAR* detector with the PEP-II asymmetric B factory. An additional 12 fb^{-1} of data taken at a center-of-mass (CM) energy 40 MeV below the $\Upsilon(4S)$ mass was used for background studies. The *BABAR* detector is described in detail elsewhere [3]. Tracking of charged particles is provided by a five-layer silicon vertex tracker (SVT) and a 40-layer drift chamber (DCH). Their identification exploits ionization energy loss in the DCH and SVT, and Cherenkov photons detected in a ring-imaging detector (DIRC). An electromagnetic calorimeter (EMC), comprised of 6580 thallium-doped CsI crystals, is used to identify electrons and photons. These systems are mounted inside a 1.5-T solenoidal superconducting magnet. Finally, the Instrumented Flux Return (IFR) of the magnet allows discrimination of muons from other particles. We use the GEANT4 Monte Carlo (MC) [4] to simulate the response of the detector, taking into account the varying accelerator and detector conditions.

3   ANALYSIS METHOD

In this analysis $B^- \to D^{*0}h^-$ candidates are reconstructed, where the *prompt* track h^- is a kaon or a pion. D^{*0} candidates are reconstructed from $D^{*0} \to D^0\pi^0$ decays and D^0 mesons from their decays to $K^-\pi^+$, $K^-\pi^+\pi^+\pi^-$, $K^-\pi^+\pi^0$, $\pi^-\pi^+$, and K^-K^+. The first three modes are referred to as "non-CP modes", while the last two as "CP modes". Reference to the charge-conjugate decays is implied here and throughout the text, unless otherwise stated.

Charged tracks used in the reconstruction of D and B meson candidates must have a distance of closest approach to the interaction point within 1.5 cm in the transverse plane and within 10

cm along the beam axis. Charged tracks from the $D^0 \to \pi^- \pi^+$ decay must also have transverse momenta > 0.1 GeV/c and total momenta in the CM frame > 0.25 GeV/c. Kaon and pion candidates from all D^0 decays must pass particle identification (PID) selection criteria based on a neural network algorithm, which uses measurements of dE/dx in the DCH and the SVT and Cherenkov photons in the DIRC.

For the prompt track to be identified as a pion or a kaon, we require that its Cherenkov angle (θ_C) be reconstructed with at least five photons. To suppress misreconstructed tracks, while maintaining high efficiency, events with prompt tracks with $\theta_C > 2$ standard deviations (s.d.) away from the expected values for both the kaon and pion hypothesis are discarded; this selection rejects most protons as well. The track is also discarded if it is identified with high probability as an electron or a muon.

Neutral pions are reconstructed by combining pairs of photons, with energy deposits larger than 30 MeV in the calorimeter that are not matched to charged tracks. The $\gamma\gamma$ invariant mass is required to be in the range 122–146 MeV/c^2. The mass resolution for all neutral pions is typically 6–7 MeV/c^2. The minimum total laboratory energy required for the $\gamma\gamma$ combinations is set to 200 MeV for π^0 candidates from D^0 mesons. Only π^0 candidates with CM momenta in the range 70–450 MeV (which we will call soft pions, π_s) are used to reconstruct the D^{*0}. A fit is performed to constrain the $\gamma\gamma$ mass to the nominal π^0 mass [5].

The D^0 mass resolution is 11 MeV/c^2 for the $D^0 \to K^- \pi^+ \pi^0$ mode and about 7 MeV/c^2 for all other modes. A mass-constrained fit is applied to the D candidate. The resolution of the difference between the masses of the D^{*0} and the daughter D^0 candidates (ΔM) is typically in the range 0.8–1.0 MeV/c^2, depending on the D^0 decay mode. A combined cut on the measured D^0 and soft pion invariant masses and on ΔM is also applied by means of a χ^2 defined as:

$$\chi^2 \equiv \frac{(m_{D^0} - \overline{m}_{D^0})^2}{\sigma^2_{m_{D^0}}} + \frac{(m_{\pi_s} - \overline{m}_{\pi_s})^2}{\sigma^2_{m_{\pi_s}}} + \frac{(\Delta M - \overline{\Delta M})^2}{\sigma^2_{\Delta M}},$$

where the mean values ($\overline{m}_{D^0}$, $\overline{m}_{\pi_s}$, $\overline{\Delta M}$) and the resolutions ($\sigma_{m_{D^0}}$, $\sigma_{m_{\pi_s}}$, $\sigma_{\Delta M}$) are measured in the data. Correlations between the χ^2 observables are negligible. Events with $\chi^2 > 9$ are rejected.

B meson candidates are reconstructed by combining a D^{*0} candidate with a high momentum charged track. For the non-CP modes, the charge of the prompt track h must match that of the kaon from the D^0 meson decay. Two quantities are used to discriminate between signal and background: the beam-energy-substituted mass $m_{\mathrm{ES}} \equiv \sqrt{(E_i^{*2}/2 + \mathbf{p}_i \cdot \mathbf{p}_B)^2 / E_i^2 - p_B^2}$ and the energy difference $\Delta E \equiv E_B^* - E_i^*/2$, where the subscripts i and B refer to the initial $e^+ e^-$ system and the B candidate respectively, and the asterisk denotes the CM frame.

The m_{ES} distribution for $B^- \to D^{*0} h^-$ signal can be described by a Gaussian function centered at the B mass and *does not* depend on the nature of the prompt track. Its resolution (about 2.6 MeV/c^2) is dominated by the uncertainty of the beam energy and is slightly dependent on the D^0 decay mode. ΔE *does* depend on the mass assigned to the tracks forming the B candidate, and on the D^0 momentum resolution. The mass hypothesis of the prompt track used to calculate ΔE is denoted by a subscript ΔE_h, where $h = \pi$ or K. ΔE_K is described approximately by a Gaussian centered at zero and with resolution 17–18 MeV, whereas ΔE_π is shifted negatively by about 50 MeV. B candidates with m_{ES} in the range 5.2–5.3 GeV/c^2 and with ΔE_K in the range (-100 to 130) MeV are selected.

Multiple candidates are found in about 10–12% of the selected events with two and four-body D^0 decays and in 17% of the events with $D^0 \to K^- \pi^+ \pi^0$ decays. The best candidate in each event is selected based on the χ^2 previously defined.

9

A large fraction of the background consists of *continuum* (non $B\overline{B}$) events; a powerful set of selection criteria is needed to suppress it. The selection is optimized to maximize the significance of the results. In the CM frame, this background typically has two-jet structure, while $B\overline{B}$ events are isotropic. We define θ_T as the angle between the thrust axes of the B candidate and of the remaining charged and neutral particles in the event, both evaluated in the CM frame, and signed so that its component along the e^- beam direction is positive. $|\cos\theta_T|$ is strongly peaked near 1 for continuum events and is approximately uniformly distributed for $B\overline{B}$ events. For the non-CP modes, $|\cos\theta_T|$ is required to be < 0.9 for the $D^0 \to K^-\pi^+$ mode, and < 0.85 for $D^0 \to K^-\pi^+\pi^+\pi^-$ and $D^0 \to K^-\pi^+\pi^0$ modes for which the levels of the continuum background are higher. For the CP modes, $\cos\theta_T$ is required to be in the ranges (-0.9 to 0.85) and (-0.85 to 0.8) for the $D^0 \to K^-K^+$ and $D^0 \to \pi^-\pi^+$ modes respectively. Other mode-dependent selection criteria are applied: events with $\cos\theta_{tD} < -0.9$ ($|\cos\theta_{tD}| > 0.95$) for $D^0 \to K^-\pi^+\pi^+\pi^-$ and $D^0 \to K^-\pi^+\pi^0$ ($D^0 \to \pi^-\pi^+$) modes are rejected, where θ_{tD} is the angle between the direction of the D^0 in the laboratory and opposite of the direction of the kaon (pion for the $D^0 \to \pi^-\pi^+$ mode) from the D^0 in the D^0 rest frame. Furthermore the momentum of the B candidate in the CM frame is required to be > 0.22 GeV/c. Finally, to reduce combinatorial background in the $D^0 \to K^-\pi^+\pi^0$ final state, only those events that fall in the enhanced regions of the Dalitz plots, according to the results of the Fermilab E691 experiment [6], are selected. The reconstruction efficiencies, based on MC simulation, are reported in Table 1.

According to the simulation, the main contributions to the $B\overline{B}$ background for $B^- \to D^{*0}h^-$ events originate from the decays $B^- \to D^{(*)0}\rho^-$ and $B^0 \to D^{*-}h^+$.

An unbinned maximum-likelihood (ML) fit is used to extract yields from the data for six candidate types, signal, continuum background and $B\overline{B}$ background, for each choice of prompt track in the candidate decays $B^- \to D^{*0}h^-$. The fit is performed independently for each D^0 decay mode.

Three quantities from each selected candidate are used as input to the fit: ΔE_K, m_{ES}, and the θ_C of the prompt track. The distributions of ΔE_K and m_{ES} for the six candidate types are parameterized to build the probability density functions (PDFs) which are used in the likelihood fit.

Correlations between the m_{ES} and ΔE_K variables for signal events are about 5% according to the simulation. To account for these, signal MC events are used to parameterize the signal PDFs using a method based on *Kernel Estimation* [7], which allows the description of a two-dimensional PDF. The shapes of MC and data distributions of these variables are in excellent agreement, although the central values are slightly shifted (more clearly for the m_{ES} distribution) by different magnitudes for the different modes. Hence the m_{ES} and ΔE_K values of the signal MC events used for the PDF for the signal are shifted accordingly before fitting the data. Systematic uncertainties associated with the statistical errors on the shifted parameters are included in the final results.

The m_{ES} PDFs for continuum background are obtained from off-resonance data with the standard selection criteria applied. The m_{ES} distributions are parameterized with an ARGUS threshold function [8]: $f(m_{ES}) \sim m_{ES}\sqrt{1-y^2}\exp\left[-\xi(1-y^2)\right]$, where $y = m_{ES}/m_0$ and m_0 is the mean energy of the beams in the CM frame. The ΔE_K PDFs for background candidates from the continuum are well parameterized with exponential functions whose parameters are determined by fitting the ΔE_K distributions of the selected $B^- \to D^{*0}h^-$ sample in the off-resonance data. Both the m_{ES} and the ΔE_K PDFs for the continuum background are taken to be the same for $B^- \to D^{*0}\pi^-$ and $B^- \to D^{*0}K^-$ decays. MC and data distributions of m_{ES} and ΔE_K obtained with looser selection criteria, in order to increase the statistics, agree well for $B^- \to D^{*0}\pi^-$ and $B^- \to D^{*0}K^-$ decays,

validating this assumption. The PDFs used for the CP modes are the same as for the $D^0 \to K^-\pi^+$ mode, as very few events from off-resonance data pass the selection criteria for these modes. This assumption is validated by comparing the distributions of m_{ES} and ΔE_K for the $D^0 \to K^-\pi^+$ and $D^0 \to K^-K^+$ or $D^0 \to \pi^-\pi^+$ modes obtained using a looser event selection.

The correlation between m_{ES} and ΔE_K for the $B\overline{B}$ background is taken into account with a two-dimensional PDF determined from simulated events, in a similar way to that used for the signal.

The PID PDFs for the kaon and pion hypotheses of the prompt track are determined from distributions, in bins of momentum and polar angle, of the difference between the reconstructed and expected θ_C of kaons and pions from D^0 decays in a control sample which exploits the decay chain $D^{*+} \to D^0\pi^+$, $D^0 \to K^-\pi^+$ to kinematically identify the tracks.

Initial PDFs are parameterized for each candidate type as described above. These do not describe exactly all the distributions of the observables used in the fit and all their correlations. This is in part caused by residual particle misidentification of the prompt tracks due to long and small non-gaussian tails in the θ_C residual distributions not removed by the prompt track selection. Hence, we use corrected PDFs for each candidate type which are weighted sums of all the initial PDFs. The weights are determined by fitting pure samples of simulated signal events and of background from off-resonance real and MC data. The corrections affecting the signal yields are typically of order 1%. The fractional systematic uncertainties for the signal yields associated to these corrections are in the range 0.1–6.0% depending on the D^0 decay mode.

The likelihood $\mathcal{L}$ for the selected sample is given by the product of the final PDFs for each individual candidate and a Poisson factor:

$$\mathcal{L} \equiv \frac{e^{-N'}(N')^N}{N!} \prod_{i=1}^{N} \sum_{j=1}^{6} \frac{N_j}{N'} \mathcal{P}_j^i(m_{ES}, \Delta E_K, \theta_C)$$

where N is the total number of events, N_j are the yields for each of the previously defined six candidate types, and $N' \equiv \sum_{j=1}^{6} N_j$, $\mathcal{P}_j^i(m_{ES}, \Delta E_K, \theta_C)$ is the probability to measure the particular set of physical quantities (m_{ES},ΔE_K,θ_C) in the ith event for a candidate of type j. The Poisson factor is the probability of observing N total events when N' are expected. The quantity $\mathcal{L}$ is maximized with respect to the six yields using MINUIT [9]. The fit has also been performed on luminosity weighted MC and high statistics toy MC events and it has been found to be unbiased. The yields thus found are corrected to account for small differences in resolutions for ΔE_K and m_{ES} between data and simulation in the parameterization of the signal.

The preliminary results of the fit are reported in detail in Table 1. These yields are used to determine the CP asymmetry parameters. We measure:

$$
\begin{aligned}
R^*_{CP+} &= 0.088 \pm 0.021(\mathrm{stat})^{+0.007}_{-0.005}(\mathrm{syst}), \\
R^*_{\mathrm{non}-CP} &= 0.0805 \pm 0.0040(\mathrm{stat})^{+0.0039}_{-0.0032}(\mathrm{syst}), \\
R^*_{CP+}/R^*_{\mathrm{non}-CP} &= 1.09 \pm 0.26(\mathrm{stat})^{+0.10}_{-0.08}(\mathrm{syst}), \\
A^*_{CP+} &= -0.02 \pm 0.24(\mathrm{stat}) \pm 0.05(\mathrm{syst}).
\end{aligned}
$$

Figure 1 shows the distributions of ΔE_K for the combined non-CP and CP modes before and after enhancing the $B \to D^{*0}K$ component. This is accomplished by requiring that the prompt track be consistent with the kaon hypothesis and that $m_{\mathrm{ES}} > 5.27\,\mathrm{GeV}/c^2$. The ΔE_K projections of the fit results are also shown.

Table 1: Results of the yields from the ML fit. For the CP modes the results of the fit separately for the B^+ and B^- samples are also quoted. Errors are statistical only. The efficiencies (ϵ) according to MC simulation are also reported.

D^0 mode	$N(B \to D^{*0}\pi)$	$N(B \to D^{*0}K)$	ε (%)
$K^-\pi^+$	2502 ± 55	218 ± 17	17
$K^-\pi^+\pi^+\pi^-$	3105 ± 66	231 ± 20	6
$K^-\pi^+\pi^0$	2984 ± 63	230 ± 21	10
K^-K^+	245 ± 18	21.4 ± 5.2	15
K^-K^+ $[B^+]$	117 ± 13	11.6 ± 3.9	15
K^-K^+ $[B^-]$	126 ± 13	9.8 ± 3.7	15
$\pi^-\pi^+$	115 ± 14	7.4 ± 4.6	13
$\pi^-\pi^+$ $[B^+]$	67 ± 11	1.8 ± 3.0	13
$\pi^-\pi^+$ $[B^-]$	46 ± 9	5.4 ± 3.5	13

The ratio of the decay rates for $B^- \to D^{*0}\pi^-$ and $B^- \to D^{*0}K^-$ is separately calculated for the different D^0 decay channels and is computed with the signal yields estimated with the ML fit and listed in Table 1. The resulting ratios are scaled by a correction factor of the order of a few percent, which is estimated with simulated data, and takes into account small differences in the efficiency between $B^- \to D^{*0}K^-$ and $B^- \to D^{*0}\pi^-$ event selections. The results are listed in Table 2.

Table 2: Measured ratios for different D^0 decay modes. The first error is statistical, the second is systematic.

$B^- \to D^{*0}h^-$ Mode	$\mathcal{B}(B \to D^{*0}K)/\mathcal{B}(B \to D^{*0}\pi)$ (%)
$D^0 \to K^-\pi^+$	$9.10 \pm 0.74^{+0.41}_{-0.32}$
$D^0 \to K^-\pi^+\pi^+\pi^-$	$7.44 \pm 0.65^{+0.32}_{-0.29}$
$D^0 \to K^-\pi^+\pi^0$	$7.73 \pm 0.71^{+0.62}_{-0.60}$
Weighted Mean (non-CP)	$8.05 \pm 0.40^{+0.39}_{-0.32}$
$D^0 \to K^-K^+$	$9.0 \pm 2.3^{+0.5}_{-0.4}$
$D^0 \to \pi^-\pi^+$	$7.5 \pm 4.8^{+1.4}_{-1.2}$
Weighted Mean (CP)	$8.8 \pm 2.1^{+0.7}_{-0.5}$

4   SYSTEMATIC STUDIES

The sources of systematic uncertainties for the yields have been identified and their contributions (for the measurement of $R^*_{(\mathrm{non}-)CP}$) are reported in Table 3. Uncertainties of the signal parameterizations of ΔE_K and m_{ES} arise from the assumed shapes of the PDFs and discrepancies between real and simulated data; all the parameters of the ΔE_K and m_{ES} PDFs have also been varied according to their statistical uncertainties (one s.d.) and the variations in the yields are taken (with their
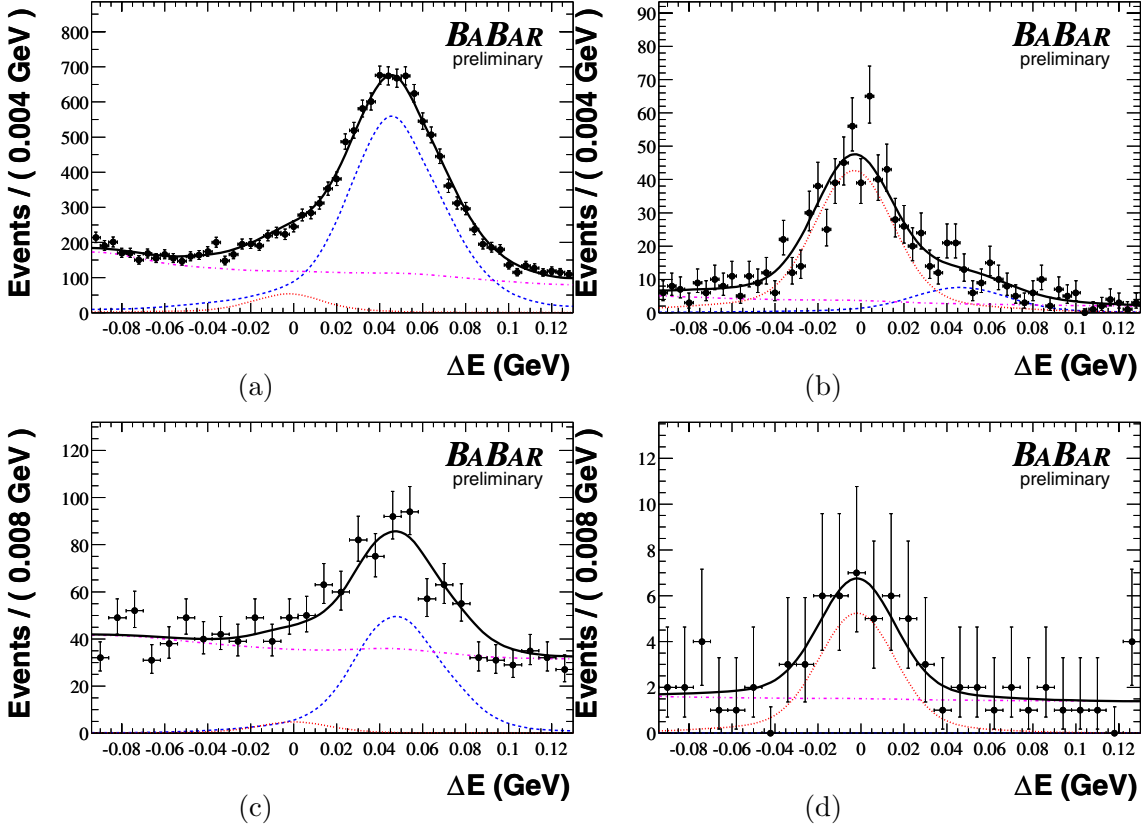
Figure 1: Distributions of ΔE_K in the $B \to D^{*0}h$ sample, for $D^0 \to K^-\pi^+, K^-\pi^+\pi^0, K^-\pi^+\pi^+\pi^-$ (top, (a), (b)) and $D^0 \to K^-K^+, \pi^-\pi^+$ (bottom, (c), (d)), before (left, (a), (c)) and after (right, (b), (d)) enhancing the $B \to D^{*0}K$ component by requiring that the prompt track be consistent with the kaon hypothesis and $m_{ES} > 5.27\,\mathrm{GeV}/c^2$. The $B^- \to D^{*0}\pi^-$ signal contribution on the right of each plot is shown as a dashed line, the $B^- \to D^{*0}K^-$ signal on the left as a dotted line, and the background as a dashed-dotted line. The total fit with all the contributions is shown with a thick solid line.

signs) as systematic uncertainties. For the $B\overline{B}$ and continuum background, the systematic uncertainties due to limited statistics of the MC and off-resonance data have been calculated varying the ΔE_K and m_{ES} PDF by their statistical uncertainties. There are several contributions to the PID systematic uncertainty for the prompt track: the uncertainty due to limited statistics is calculated by varying each parameter of the PDF in each bin in momentum and polar angle by its uncertainty (keeping constant all other parameters in the same bin and all parameters in all the other bins) and summing all the contributions in quadrature; results obtained with alternative PID PDFs, which account for different θ_C residual shapes and for discrepancies between data and simulation, are also included as systematic uncertainties. The systematic uncertainties due to the PDF reweighting procedure have been evaluated. Finally, errors associated to the efficiency correction factor are also included.

Many of the systematic uncertainties for the signal yields have similar effects on the $B^- \to D^{*0}K^-$ and $B^- \to D^{*0}\pi^-$ events (they increase or decrease both fractions simultaneously), hence

their effect is reduced in deriving the systematic uncertainty for the measurement of the ratios, when all correlations are taken into account. Overall, the main sources of systematic uncertainties for the measurement of both $R^*_{(non-)CP}$ and A^*_{CP+} are due to the characterization of the shapes of m_{ES} and ΔE_K for the signal, to the characterization of the m_{ES} PDFs for the background, to the particle identification, and to the uncertainty of the PDFs weighting procedure and of the efficiency correction factors. The systematic uncertainty for A^*_{CP+} due to possible detector charge asymmetries is evaluated by measuring asymmetries analogous to those defined in Eq. 1, but for $B^- \to D^{*0}\pi^-$ and $B^- \to D^{*0}K^-$ events (the latter uniquely for the non-CP modes), where CP violation is expected to be negligible. Results for all modes are then combined, taking correlations into account. The measured asymmetry is $-0.010 \pm 0.012(\text{stat})^{+0.002}_{-0.001}(\text{syst})$ and its maximum variation from zero up to one s.d. (0.022) is taken, conservatively, as a further symmetric systematic error on A^*_{CP+}. When combining the results for the different modes, all systematic and statistical uncertainties are considered to be uncorrelated, except for the contributions of the PID PDF (common to all modes) and of the detector charge asymmetry in the measurement of A^*_{CP+}, which are considered to be completely correlated. For the measurement of $R^*_{CP+}/R^*_{\text{non}-CP}$ all systematic uncertainties have been considered to be uncorrelated; this assumption is conservative, and has negligible effect on the largely statistically limited final result.

Table 3: Average systematic uncertainties for $R^*_{(\text{non})-CP}$.

Systematic Source	$R^*_{\text{non}-CP}$ $\Delta R^*_{\text{non}-CP}/R^*_{\text{non}-CP}(\%)$ non-CP modes	R^*_{CP} $\Delta R^*_{CP}/R^*_{CP}(\%)$ CP modes
ΔE_K (signal)	$+1.9$ -1.8	$+2.4$ -2.3
$\Delta E_K(q\bar{q})$	$+0.3$ -0.4	$+1.5$ -2.2
$\Delta E_K(B\bar{B})$	$+0.2$ -0.4	$+1.1$ -1.7
m_{ES} (signal)	$+0.4$ -0.3	$+0.6$ -0.7
m_{ES} $(q\bar{q})$	$+0.9$ -0.9	$+4.9$ -2.1
m_{ES} $(B\bar{B})$	$+1.5$ -1.6	$+3.4$ -3.3
PDF Weights	$+2.7$ -2.7	$+1.0$ -1.2
PID PDF	$+2.7$ -1.8	$+2.2$ -2.0
ε Correction	$+1.5$ -1.5	$+2.0$ -2.0

5 SUMMARY

In conclusion, we have measured the ratio of the decay rates for $\mathcal{B}(B^- \to D^{*0}K^-)$ and $\mathcal{B}(B^- \to D^{*0}\pi^-)$, with non-$CP$ eigenstates. This constitutes the most precise measurement of this kind. We have also performed the first measurement of the same ratio and of the CP asymmetry A^*_{CP+} for D^0 mesons decaying to CP eigenstates. These results, together with measurements exploiting $B^- \to D^0K^-$, $B^- \to D^0K^{*-}$ and $B^- \to D^{*0}K^{*-}$ decays [2, 10], constitute a first step towards measuring the angle γ. All the results presented in this document are preliminary. Assuming factorization and flavor-SU(3) symmetry, theoretical calculations (in the tree-level approximation) predict: $\mathcal{B}(B^- \to D^{*0}K^-)/\mathcal{B}(B^- \to D^{*0}\pi^-) \sim (V_{us}/V_{ud})^2(f_K/f_\pi)^2 \sim 0.074$, where f_K and f_π are

the meson decays constants [11]. Our results accord with these predictions.

6   ACKNOWLEDGMENTS

References

[1] M. Gronau and D. Wyler, Phys. Lett. B **265**, 172 (1991); M. Gronau and D. London, Phys. Lett. B **253**, 483 (1991); D. Atwood, I. Dunietz and A. Soni, Phys. Rev. Lett. **78**, 3257 (1997); A. Soffer, Phys. Rev. D **60**, 054032 (1999); M. Gronau, Phys. Rev. D **58**, 073301 (1998); Z. Xing, Phys. Rev. D **58**, 093005 (1998); J.H. Jang and P. Ko, Phys. Rev. D **58**, 111302 (1998); M. Gronau and J.L. Rosner, Phys. Lett. B **439**, 171 (1998).

[2] Belle Collaboration, K. Abe *et al.*, Phys. Rev. Lett. **87**, 111801 (2001).

[3] *BABAR* Collaboration, B. Aubert *et al.*, Nucl. Instr. and Methods **A479**, 1 (2002).

[4] GEANT4 Collaboration, S. Agostinelli *et al.*, Nucl. Instr. and Methods **A506**, 250 (2003).

[5] Particle Data Group, K. Hagiwara *et al.*, Phys. Rev. D **66**, 010001 (2002)

[6] E691 Collaboration, J. C. Anjos *et al.*, Phys. Rev. D **48**, 56 (1993)

[7] K. S. Cranmer, Comp. Phys. Commun. **136**, 198 (2001).

[8] ARGUS Collaboration, H. Albrecht *et al.*, Z. Phys. **C48**, 543 (1990)

[9] F. James, Comput. Phys. Commun. **10**, 343 (1975).

[10] *BABAR* Collaboration, B. Aubert *et al.*, Phys. Rev. D **69**, 051101 (2004); *BABAR* Collaboration, B. Aubert *et al.*, Phys. Rev. Lett. **92**, 202002 (2004); *BABAR* Collaboration, B. Aubert *et al.*, Phys. Rev. Lett. **92** 141801 (2004); Belle Collaboration, S.K. Swain *et al.*, Phys. Rev. D **68**, 051101 (2003).

[11] M Gronau *et al.*, Phys. Rev. D **52**, 6356 (1995).